

# Influence of a nanometric Al<sub>2</sub>O<sub>3</sub> interlayer on the Thermal Conductance of an Al/(Si,Diamond) interface

---

By *Christian Monachon\**, and *Ludger Weber*

[\*] *Dr Christian Monachon Corresponding-Author, Dr. Ludger Weber Author-Two  
Laboratoire de Métallurgie Mécanique  
École Polytechnique Fédérale de Lausanne, 1015 Lausanne, Switzerland  
E-mail: christian.monachon@gmail.com*

[\*\*] *Financial support of C. Monachon by the SNSF Project No. 200021-121881 and 200020-135132 is gratefully acknowledged. Didier Bouvet of the EPFL Center for MicroNanotechnology is acknowledged for his help in the ALD layers deposition. Prof Hubert Girault of the Laboratoire d'Électrochimie Physique et Analytique (LEPA) at EPFL is acknowledged for providing the laser source for the experiments. Prof David G. Cahill of the University of Illinois at Urbana Champaign is gratefully acknowledged for helpful discussions.*

## Abstract

The effect of an Al<sub>2</sub>O<sub>3</sub> interlayer on the thermal conductance of metal (Al) / non-metal (diamond and silicon) interfaces is investigated using Time Domain ThermoReflectance (TDTR). Interlayers between 1.7 and 20 nm are deposited on oxygen-terminated diamond and hydrogen-terminated silicon substrates using Atomic Layer Deposition (ALD). Their overall conductance is then measured at temperatures ranging from 78 to 290 K. The contributions of the interlayer bulk and its interfaces with both substrate and metallic overlayer are then separated. Values thus obtained for the bulk interlayer conductivity are comparable with existing data, reaching 1.25 Wm<sup>-1</sup>K<sup>-1</sup> at 290 K. Interface contributions are shown to be very similar to the values obtained when a single Al/substrate interface is investigated, suggesting that interfacial oxides may govern TBC independently of the interlayer's thickness.

## 1. Introduction

The finite Thermal Boundary Conductance (TBC) between metals and dielectrics has attracted an increasing interest in recent years because at the nanoscale, interfaces are becoming non-negligible limiters of heat transfer.<sup>[1]</sup> Indeed, the use of ever increasing circuitry density in chips and processors leads to an accordingly increasing heat generation density, which has to be evacuated through a correspondingly higher maze of resistive interfaces.<sup>[2]</sup> On the other hand, a finite TBC can also be used as a tool to decrease the overall thermal conductivity of a multilayer material.<sup>[3, 4]</sup> The TBC is additionally an important factor in the calculation of the heat conduction of superlattices<sup>[5, 6]</sup> even though recent evidence shows that for highly ordered superlattices, coherent phonon transport may balance the influence of interfaces.<sup>[7]</sup> Compared to early measurements in cryogenic conditions on macroscopic samples<sup>[8]</sup>, advances in characterization techniques have enabled conductances to be measured experimentally on an increasing variety of interfaces<sup>[9-13]</sup>, and also at higher temperatures. So far, the measured data, especially at high temperatures, have mostly been an unresolved challenge for existing models.<sup>[8, 14, 15]</sup> Measured TBCs can be much higher than predicted, especially if the phonon spectrum of the two materials in contact is highly mismatched, as is the case with Au- or Pb-diamond interfaces.<sup>[9, 12]</sup>

Many modifications to the Acoustic<sup>[14]</sup> and Diffuse<sup>[8]</sup> Mismatch Models have therefore been proposed to account for the observed differences between existing models and experiments. Typically these modifications involve the addition of a scattering parameter<sup>[16]</sup>, consideration of interfacial states<sup>[17]</sup>, and bond strength<sup>[18]</sup>, or of many-phonons processes.<sup>[19]</sup> Other models consider the contribution of electrons to heat transfer between metals and dielectrics,<sup>[20, 21]</sup> but experimental evidence from Stoner and Maris<sup>[9]</sup> and Lyo and Cahill<sup>[12]</sup> on the Pb-diamond

system suggest that electrons take a negligible part in heat transfer at metal/dielectric interfaces. Furthermore, molecular dynamics (MD) simulation by Choi *et al.*<sup>[22]</sup> suggest that this effect may be negligible. More complex MD approaches<sup>[22-28]</sup> have been developed and seem promising, but except for one based on Density Functional Theory (DFT)<sup>[22]</sup>, empirical potentials are used and their results, however useful qualitatively, must be taken with caution. A further approach consists in using a Green's function formalism, either with harmonic interatomic potentials<sup>[29]</sup> or with potentials calculated using first-principles methods<sup>[27, 30]</sup>. The ability of this last method to account efficiently for an interfacial stiffness different from the bulk<sup>[31]</sup> or the presence of foreign atoms at the interface<sup>[32, 33]</sup> makes it a promising method to calculate TBCs in real systems. Its main drawback is the computational cost of calculating real interatomic potentials.

On the experimental side, relatively few contributions exist showing the effect of an interfacial layer on a metal/dielectric TBC, the noticeable examples consisting of polymer layers<sup>[31, 34, 35]</sup>, silicides<sup>[36, 37]</sup>, oxides<sup>[38, 39]</sup>, or an additional metal layer.<sup>[40]</sup> In the past few years Al<sub>2</sub>O<sub>3</sub> layers deposited on silicon by Atomic Layer Deposition (ALD) have gathered interest for several potential applications. Indeed, ALD is viewed as a potential replacement high-k material for SiO<sub>2</sub> or SiO<sub>2</sub>/SiN<sub>x</sub>/SiO<sub>2</sub> in Complementary Metal-Oxide-Semiconductor (CMOS) technology and other transistor technologies.<sup>[41-44]</sup> It is also a good candidate for surface passivation layers in solar cells<sup>[45-47]</sup>, especially the passivated emitter rear locally diffused cells. It is further successfully used to encapsulate organic electronic devices<sup>[48-50]</sup> and is expected to help improve the lifetime of Li-Ion batteries.<sup>[51]</sup> While much effort has been put into describing its electric, mechanical, chemical and diffusion properties of ALD alumina, only little effort has been made to characterize its thermal properties.<sup>[52]</sup> This knowledge could be relevant because the miniaturization of microelectronics increases significantly the criticality of thermal management. In a previous study, Lee *et al.*<sup>[53]</sup> characterized the thermal conductivity of various sputtered amorphous Al<sub>2</sub>O<sub>3</sub> thin films

using the  $3\omega$  method<sup>[54]</sup> and found that their conductivity could vary by as much as a factor of two depending on the sputtering technique. However, they worked with relatively thick films, in the 0.5-2  $\mu\text{m}$  range, which impairs the measurement of interface conductances. It can be anticipated that these latter conductances will be responsible for an increasing fraction of the overall thermal barrier imposed by the film when its thickness diminishes, motivating the present contribution, in which the effect of a nm-sized  $\text{Al}_2\text{O}_3$  interlayer on the conductance at Al/diamond and Al/Si interface is investigated. Specifically, layers of 1.7, 4.5, 6.7, 10 and 20 nm of amorphous  $\text{Al}_2\text{O}_3$  are deposited on diamond and silicon substrates by ALD, and are then covered with an 140 nm thick Al overlayer. The obtained samples are then investigated using Time Domain ThermoReflectance. The aims of these measurements are twofold: i) to measure the interface contribution of the conductance of this interlayer as a function of its thickness and temperature, and ii) to provide thermal conductivity data of nm-sized amorphous  $\text{Al}_2\text{O}_3$  layers.

## 2. Experimental

### 2.1. Sample preparation

Clean, oxygen-terminated monocrystalline diamond substrates were produced by exposing [100]-oriented diamonds to an Ar:O plasma in a Fischione model 1020 plasma cleaner. Clean, hydrogen-terminated silicon substrates were prepared by dipping a [100]-oriented wafer in a conventional buffered HF: $\text{NH}_4\text{F}$  (1:6) solution.  $\text{Al}_2\text{O}_3$  layers of nominally 1, 3, 5, 10 and 20 nm were then deposited by ALD using a BENEQ TFS200 apparatus (Beneq Oy, Vantaa, Finland, deposition temperature: 200 °C). The samples were then re-exposed to the Ar:O plasma and transferred to a Balzers BAS 450 DC sputter deposition system in which a 140 nm Al layer was deposited at a speed of  $6 \text{ \AA s}^{-1}$  over all samples.

### 2.2. Transmission Electron Microscopy

TEM cross-section lamellae were prepared using a Zeiss NVision 40 FIB to verify the layer thicknesses on the diamond substrates with 1, 3, 5 and 10 nm layers. TEM samples were prepared from the Si substrate samples using conventional tripod polishing followed by a light ion bombardment. These samples were imaged using a FEI CM300 High Resolution Transmission Electron Microscope (HRTEM).

### 2.3. Time Domain ThermoReflectance

#### 2.3.1. Setup

TDTR experiments were performed using a setup described elsewhere in detail.<sup>[55]</sup> In a nutshell, it uses a Spectra Physics Tsunami laser producing 200 fs pulses at a repetition rate of 80 MHz and a wavelength of 790 nm. Its beam is split into two parts, the pump and the probe. The pump is modulated at 10.7 MHz using an electro-optic modulator (EOM) and passes through a mechanical delay stage which can create a delay of up to 4 ns between pump and probe pulses. After being filtered to differentiate their wavelength<sup>[56]</sup>, both pump and probe beams are focused to overlapping spots of about  $5 \mu\text{m}$   $e^{-2}$  radius using a microscope objective. The fluences used range between 0.1 (at low T) and  $0.3 \text{ mJcm}^{-2}$ , leading to temperature rises below 1 K in the metal layer. Steady-state heating of the samples was also estimated to be below 1 K using the formula derived by Cahill.<sup>[57]</sup> The reflection of the probe from the sample (which is schematically represented *e.g.* for a diamond substrate in **Figure 2(d)**) is sent to a fast photodiode, the signal of which is filtered, pre-amplified, and sent to a lock-in amplifier (LOA), which is also used to generate the modulating signal for the EOM. By measuring the signal in the photodiode at various delay times, a cooling curve of the sample surface over at maximum 4 ns delay is obtained. The ratio of the in-phase (X) and out-of-phase (Y) signals from the LOA are fitted using an analytical model first developed by Cahill.<sup>[57]</sup> It consists in using the approach for a frequency domain solution and to extend it to an analytical solution of the heat flow in layered structure developed by

Feldman<sup>[58]</sup>. Indeed, taking the Hankel transforms<sup>[59]</sup> of the gaussian power distribution of the pump and the probe beams (of  $e^{-2}$  size  $w_0$  and  $w_1$  respectively), they can be convoluted in the  $k$  domain to get a solution of the form:

$$\Delta T = 2\pi A \int_0^\infty G(k) e^{-\pi^2 k^2 \frac{w_0^2 + w_1^2}{2}} k dk \quad (1)$$

with  $A$  the power of the pump beam and  $G(k)$  the Hankel Transform of the frequency-domain solution of the heat transfer problem of interest. This integral over  $k$  can be truncated at about  $2(w_0^2 + w_1^2)^{1/2}$  without a large loss of accuracy<sup>[57]</sup>. Feldman<sup>[58]</sup> proposed an algorithm to find an analytical solution for  $G(k)$  in a layered structure. It consists in first defining temperature coefficients  $B$  for the forward and backward propagating waves for each layer<sup>[60]</sup>:

$$u_n = \sqrt{4\pi^2 k^2 + \frac{i\omega C_n}{k_n}} \quad (2)$$

$$\Gamma_n = k_n u_n \quad (3)$$

$$\begin{pmatrix} B^+ \\ B^- \end{pmatrix}_n = \frac{1}{2\Gamma_n} \begin{pmatrix} e^{-u_n d_n} & 0 \\ 0 & e^{u_n d_n} \end{pmatrix} \begin{pmatrix} \Gamma_n + \Gamma_{n+1} & \Gamma_n - \Gamma_{n+1} \\ \Gamma_n - \Gamma_{n+1} & \Gamma_n + \Gamma_{n+1} \end{pmatrix} \begin{pmatrix} B^+ \\ B^- \end{pmatrix}_{n+1} \quad (4)$$

with  $d_n$ ,  $C_n$  and  $\kappa_n$  respectively the thickness, volumetric heat capacity and heat conductivity of the  $n$ -th layer. Using Equations (2) to (4) starting from the bottom layer –the substrate– and assuming that in the timescale of interest, heat cannot reach the bottom of the layer (*i.e.*  $B^+ = 0$ ,  $B^- = 1$ ), the values for  $B^+$  and  $B^-$  at the top layer –the metallic film– can be calculated. A Boundary conductance can be modeled using a very thin layer with a heat capacity close to zero. Using Equations 3 and 4  $G(k)$  is then:

$$G(k) = \frac{1}{\Gamma_1} \begin{pmatrix} B_1^+ + B_1^- \\ B_1^- - B_1^+ \end{pmatrix} \quad (5)$$

Equation (5) can then be combined with Equation (1) to accurately describe the frequency

domain solution of the layered system. To calculate the response as a function of the time delay, each laser pulse, being much shorter than the period  $P$  between the pulses, can be considered as instantaneous. Since the pump beam is modulated at frequency  $f$  and the lock-in amplifier picks the frequency components at  $\pm f$ , the delay time  $t$  is treated as a phase component equal to zero at  $t = 0$  and  $t = P$ . These statements are expressed as follows<sup>[57]</sup>:

$$Re[\Delta R_M(t)] = \frac{dR}{dT} \sum_{m=-M}^M \left( \Delta T \left( \frac{m}{P} + f \right) + \Delta T \left( \frac{m}{P} - f \right) \right) e^{i2\pi m t/P} \quad (6)$$

$$Im[\Delta R_M(t)] = -i \frac{dR}{dT} \sum_{m=-M}^M \left( \Delta T \left( \frac{m}{P} + f \right) - \Delta T \left( \frac{m}{P} - f \right) \right) e^{i2\pi m t/P} \quad (7)$$

with  $\frac{dR}{dT}$  a factor containing the thermoreflectance coefficient and the gain of the electronic circuit. In an ideal case,  $M$  should be set to  $\infty$  but in any practical case taking  $M = 10Pt_{min}^{-1}$ , where  $t_{min}$  is the minimum time delay considered, gives sufficient accuracy provided that the convergence of the sum in the real part is hastened by a factor of the form  $e^{-\pi(f t_{min}/10)}$ .

The heat capacities used in the model of Al, Si and diamond were taken from Touloukian<sup>[61]</sup>.

The same source was used for the thermal conductivities of Al and Si. The thermal conductivity of diamond was taken from Hudson<sup>[62]</sup>.

### 2.3.2. $Al_2O_3$ layer intrinsic thermal conductivity measurement

Sensitivities,  $S_{i(T)}$ , to the model used to extract thermal properties are calculated as follows:

$$S_{i(T)} = \left| \frac{\partial \ln \left[ \frac{X(t,T)}{Y(t,T)} \right]}{\partial \ln [i(T)]} \right| \quad (8)$$

with  $i$  the parameter of interest, in our case the conductivity  $k$  and volumetric heat capacity  $C$ ,  $t$  the delay time between pump and probe, and  $T$  the temperature. The calculation is performed using the thermal conductivities measured by Lee *et al.*<sup>[63]</sup> and the heat capacity of sapphire from Touloukian.<sup>[61]</sup> The thermal conductivity used in the model is assumed isotropic since

the frequencies used are high, yielding identical results in a 1D or axially symmetric model.<sup>[60]</sup>

Sample surface cooling curves are measured by TDTR at temperatures between 78 and 290 K using an optical cryostat cooled by liquid nitrogen. The results for the conductivity of the Al<sub>2</sub>O<sub>3</sub> interlayer are then calculated by fitting the X/Y ratio of the obtained curves using Equ. (6) and (7). The parameters allowed to vary are the conductivity of the Al<sub>2</sub>O<sub>3</sub> layer and that of the substrate since very small spot sizes are used, which is known to significantly reduce the measured conductivity of solids with mean free paths longer than the spot size.<sup>[33, 64]</sup> After measuring the apparent thermal conductivity  $k_{app}$  of the Al<sub>2</sub>O<sub>3</sub> layer at each thickness  $d$ , the inverse of its equivalent apparent stack conductance,  $h^{-1}$ , is plotted against the thickness:

$$h_{app} = \frac{d}{k_{app}} = \frac{d}{k_{int}} + \frac{1}{h_{bd}} \quad (9)$$

Using this relation and fitting the obtained points with a regression curve, the slope of the curve is the inverse of the intrinsic thermal conductivity of the layer,  $k_{int}$ , and its regression to zero is the inverse of the contribution of interfaces,  $h_{bd}$ . The error  $\sigma$  on the values obtained this way are then calculated as follows<sup>[65]</sup>:

$$\sigma(k_{int}^{-1}) = k_{int}^{-1} \frac{\tan(\cos^{-1} R)}{\sqrt{N-2}} \quad (10)$$

$$\sigma(h_{bd}^{-1}) = \sigma(k_{int}^{-1})(h_{app}^{-1})_{rms} \quad (11)$$

with  $R$  the correlation coefficient of the fit and  $N$  the number of measurements.

### 3. Results

**Figure 1** shows the sensitivity analysis of the data extraction model to  $\kappa_{Al_2O_3}$  and  $C_{Al_2O_3}$ , calculated using Eq. 8. Only one example is shown for the sensitivity to  $C_{Al_2O_3}$ , because the sensitivity to heat capacity increases with interlayer thickness, so if the model was sensitive to  $C_{Al_2O_3}$ , the thickest layer investigated would show it best.



**Figure 2** shows examples of the images used to determine the exact  $\text{Al}_2\text{O}_3$  interlayer thicknesses. The contrast is better on the Si substrates because samples are thinner when prepared by tripod polishing, and the interatomic distance between Si atoms is wider, making it easier to discern atomic columns.

**Figure 3** shows examples of fits using Eq. 10 obtained on thermal resistances measured on the  $\text{Al}_2\text{O}_3$  layers on Al/ $\text{Al}_2\text{O}_3$ /Si and Al/ $\text{Al}_2\text{O}_3$ /C substrates, with respective interlayer thicknesses of 6.7, 10 and 20 nm (Al/Si) and 1.7, 4.5, 6.7 and 10 nm (Al/C). Half of the temperatures have been removed for clarity (trends are monotonic).

**Figure 4** (a) shows the values obtained for the cross-plane thermal conductivity of an  $\text{Al}_2\text{O}_3$  interlayer, compared with literature values from Lee *et al.*<sup>[63]</sup>. Figure 4 (b) shows the values obtained for Al/ $\text{Al}_2\text{O}_3$  and  $\text{Al}_2\text{O}_3$ /X (X=C,Si) interface contributions to the conductance of the  $\text{Al}_2\text{O}_3$  interlayers, compared with literature values for Al/O:C[33], Al/H:Si<sup>[64]</sup> and Al/SiO<sub>2</sub>/Si<sup>[66]</sup> interfaces.

**Figure 5** presents the same results as in **Figure 4**, except that apparent conductances  $h_{\text{app}}$  instead of conductivities  $\kappa_{\text{app}}$  were extracted using the thermal model. The heat capacity of the  $\text{Al}_2\text{O}_3$  interlayer was accounted for by artificially increasing the Al layer thickness in the fitting model. The blue lines show an extrapolation of the spline fit made on the data without ALD deposited interlayer.

## 4. Discussion

The calculated sensitivity of the data extraction model to  $\kappa_{\text{Al}_2\text{O}_3}$  and  $C_{\text{Al}_2\text{O}_3}$  shown in **Figure 1** suggests that in the timescale considered our experiment is much more sensitive to  $\kappa_{\text{Al}_2\text{O}_3}$  than to  $C_{\text{Al}_2\text{O}_3}$  (this trend would be reversed if thick (>300 nm) layers were used). We thus can use  $C_{\text{Al}_2\text{O}_3}$  of sapphire without risking an error greater than the variability of a TDTR

experiment.<sup>[55]</sup> The regions of highest sensitivity are taken into account when calculating the fits to the experimental data at each temperature.

From **Figure 2** we deduce that  $\text{Al}_2\text{O}_3$  film growth is initially faster than expected, yet even the thinnest ALD layers deposited are dense. Indeed, as a crystalline Al layer has been deposited onto the amorphous oxide layer, diffraction contrasts would inevitably be visible in a cross-sectional TEM image if the ALD layer had formed islands. The rapid initial growth rate of this continuous layer must, therefore, be caused by bonding effects, the underlying layer increasing the probability of atom bonding compared to what obtains on thick amorphous alumina. **Figure 2** (c) suggests no variation in film density throughout its thickness. Indeed, if existing, such a variation would be highlighted by a contrast in transmitted electron intensity. This fact is confirmed in *Fig. 3* by the fact that no trend departure from the linear regression at low thicknesses can be observed at most thicknesses.

Measured thermal conductivities shown in **Figure 4** (a) for both the Al/ $\text{Al}_2\text{O}_3$ /C and Al/ $\text{Al}_2\text{O}_3$ /Si systems indicate that the data can be separated into two classes:

- at temperatures above 140K, data fall approximately midway between measurements made by Lee *et al.*<sup>[63]</sup> and agree reasonably with each other. The obtained data also compare well with measurements on amorphous alumina produced by anodization<sup>[67]</sup>, as well as other data on ALD deposited thin films extrapolated to lower temperature.<sup>[52]</sup>
- below 140 K, values start to vary substantially. The large variations below 140K can be rationalized by three effects:
  1. In data extracted by a procedure like that represented in **Figure 3** for diamond substrates, the total resistance values for thin interlayers at low temperatures are largely dominated by the interface contribution, the latter dropping more rapidly with decreasing temperature than the thermal conductivity. Hence scatter in the total interface conductance measured may lead to significant

uncertainty in the slope, from which the conductivity is derived.

2. With decreasing temperature the phonon mean free path in the interlayer may become of the order of the interlayer thickness for the smallest thicknesses, which may reduce the effective conductivity of the layer. For the thermal conductivities measured without taking this effect into account, the mean free path of phonons can be evaluated to be clearly below 1 nm. According to Cahill and Pohl<sup>[68]</sup> the phonon mean free path is typically half of a wavelength far below the high temperature limit. For temperatures below 150K and elastic properties of alumina this would lead to a phonon mean free path on the order of 1 nm. Hence it cannot be excluded that including layers as thin as 1.7 nm in the linear extrapolation may slightly affect the evaluated thermal conductivity of the alumina layer, causing a linear regression fit using Eq. 2 to no longer be valid, e.g. in the curve obtained at 78 K in **Figure 3** (b).
3. At temperatures between 120 and 160 K, water vapor pressure becomes of the order of the overall pressure in the cryostat<sup>[69]</sup> (measured to be of about  $10^{-5}$  mbar during operation). Some ice may therefore have evaporated from the coolest parts of the cryostat and re-deposited on the sample's surface, changing its heat capacity and thereby its cooling response. Even though i) no ice was observed at the sample's surface using the microscope objective used to focus the laser and ii) steps such as shielding the sides of the sample using copper pieces acting as cold fingers and using clean samples surfaces to prevent ice nucleation were taken to reduce the risk of ice contamination, this possibility cannot be discarded in the event of the formation of a nm-thin, homogeneous layer.

We therefore discard thermal conductivity data obtained below 140K. Data obtained above 140 K are on the other hand coherent, confirming the approach adopted here for film

thicknesses in the range from 4 to 20 nm (and probably also for higher thicknesses, as long as the fitting model used doesn't become too sensitive to heat capacity).

If we compare the present data for interface contributions to the conductance between the Al overlayer and the substrate with literature data from Duda (Al/SiO<sub>2</sub>/Si) and from a previous contribution<sup>[33]</sup>, one finds that (Al/O:C) shows values very similar over the whole investigated temperature range. This suggests that i) the Al-O bonding at the interface is the factor enabling the high TBC observed between Al and oxygenated diamond<sup>[32, 33, 70]</sup> and ii) these interfacial oxide states should be treated in a model trying to quantify TBC, as e.g. in Ref.<sup>[29]</sup>.

To further verify this assertion without polluting the analysis with potential numerical artifacts mentioned above, in **Figure 5**, the obtained TDTR cooling curves are re-analyzed using an interfacial conductance term containing the interlayer conductivity and the conductances of both its interfaces is plotted as a function of temperature. The heat capacity  $C$  of the interlayer of thickness  $d_{\text{Al}_2\text{O}_3}$  is accounted for by artificially increasing the Al overlayer thickness by an amount equal to  $d_{\text{Al}_2\text{O}_3} C_{\text{Al}_2\text{O}_3} / C_{\text{Al}}$ . The black fitting curves of the TBCs  $h_{\text{bd},d}$  were obtained using a spline fit  $h_{\text{bd},0}$  of the Al/O:C data and by adding the stack resistance of the amorphous Al<sub>2</sub>O<sub>3</sub> layer with conductivity  $\kappa_{\text{Al}_2\text{O}_3}$  and thickness  $d_{\text{Al}_2\text{O}_3}$ :

$$h_{\text{bd},d}^{-1} = h_{\text{bd},0}^{-1} + \frac{d_{\text{Al}_2\text{O}_3}}{\kappa_{\text{Al}_2\text{O}_3}} \quad (12)$$

the conductivity values were obtained by taking the average of the maximum and minimum values of amorphous Al<sub>2</sub>O<sub>3</sub> provided by Lee *et al.*<sup>[63]</sup>, as they are more precise over the whole considered temperature range. The difference in TBC measured with and without an Al<sub>2</sub>O<sub>3</sub> interlayer is accounted for quite well using an equivalent stack conductance. The only substantial discrepancy is visible for the 1.7 nm layer at very low temperature, but this may well be due to ballistic effects within the layer, diminishing its conductivity.

Overall, the accuracy of the obtained comparison between the interface without and those with an Al<sub>2</sub>O<sub>3</sub> interlayer suggest that as far as the contribution of TBC is concerned, the Al

layer deposited on O-terminated diamond can be treated like an Al/Al<sub>2</sub>O<sub>3</sub>/diamond triple layer with a zero Al<sub>2</sub>O<sub>3</sub> layer thickness. Conversely, the boundary conductance contributions of the Al/Al<sub>2</sub>O<sub>3</sub> and the Al<sub>2</sub>O<sub>3</sub>/diamond interface are equal within experimental error to the Al/O:diamond interface contribution.

Finally, note that the presence of a layer between two materials affects the TBC between them even for an interlayer thickness as thin as 1.7 nm, a fact that is important when considering interface engineering approaches to increase TBC between materials.<sup>[22, 26, 28]</sup> Indeed, with phase velocities and Debye temperature between those of Al and diamond, Al<sub>2</sub>O<sub>3</sub> meets the criterion set by these References to improve thermal transport across the Al/diamond interface; however, its own contribution to the interface conductance is, at least in its amorphous state, non-negligible even for a nanometer-thin layer.

## 5. Conclusion

Time Domain ThermoReflectance has been used to investigate the interface conductance and bulk conductivity contributions on Atomic Layer Deposited Al<sub>2</sub>O<sub>3</sub> thin films deposited between Si or C substrates and Al overlayers. A method is presented to decouple the conductance and conductivity contributions using measurement on samples with varying interlayer thicknesses. The results obtained for the intrinsic thermal conductivity of ALD deposited Al<sub>2</sub>O<sub>3</sub> fall halfway between existing literature data, steadily increasing up to a value of  $1.25 \pm 0.15 \text{ Wm}^{-1}\text{K}^{-1}$  at ambient.

The comparison of the Al/Al<sub>2</sub>O<sub>3</sub>/C TBC values presented here with values obtained on Al/O:C in a previous contribution suggest that the presence of a monolayer of oxygen at the surface of diamond changes the way heat passes through the interface between Al and diamond by creating Al:O interfacial states. This conclusion might also hold for an Al/SiO<sub>2</sub>/Si interface as the obtained values are very close, but further experiments using a SiO<sub>2</sub> interlayer with varying thickness would be necessary to confirm this fact. Indeed, our results show that

adding amorphous  $\text{Al}_2\text{O}_3$  at the interface changes the effective measured TBC in agreement with a simple stack conductance calculation using literature values for amorphous  $\text{Al}_2\text{O}_3$  conductivity, while the contributions from the interfaces stay unchanged.

## References

- [1] D. G. Cahill, F. K. Wayne, K. E. Goodson, G. D. Mahan, A. Majumdar, H. J. Maris, R. Merlin, and S. R. Philipot, *Applied Physics Reviews*, **2003**, 93, 793.
- [2] E. Pop, *Nano Research*, **2010**, 3, 147.
- [3] R. M. Costescu, D. G. Cahill, F. H. Fabreguette, Z. A. Sechrist, and S. M. George, *Science*, **2004**, 303, 989.
- [4] C. Chiritescu, D. G. Cahill, N. Nguyen, D. Johnson, A. Bodapati, P. Keblinski, and P. Zschack, *Science*, **2007**, 315, 351.
- [5] W. S. Capinski, H. J. Maris, T. Ruf, M. Cardona, K. Ploog, and D. S. Katzer, *Physical Review B*, **1999**, 59, 8105.
- [6] C. Dames, *Nature nanotechnology*, **2012**, 7, 82.
- [7] M. N. Luckyanova, et al., *Science*, **2012**, 338, 336.
- [8] E. T. Swartz and R. O. Pohl, *Reviews of Modern Physics*, **1989**, 61, 605.
- [9] R. J. Stoner and H. J. Maris, *Physical Review B*, **1993**, 48, 16373.
- [10] S.-M. Lee and D. G. Cahill, *Microscale Thermophysical Engineering*, **1997**, 1, 47.
- [11] R. M. Costescu, M. D. Wall, and D. G. Cahill, *Physical Review B*, **2003**, 67, 1.
- [12] H.-K. Lyeo and D. G. Cahill, *Physical Review B*, **2006**, 73, 144301 1.
- [13] P. E. Hopkins, P. M. Norris, and R. J. Stevens, *Journal of Heat Transfer*, **2008**, 130, 022401.
- [14] W. A. Little, *Canadian Journal of Physics*, **1959**, 37, 334.
- [15] D. A. Young and H. J. Maris, *Physical Review B*, **1989**, 40, 3685.
- [16] R. S. Prasher and P. E. Phelan, *Journal of heat Transfer-Transactions of the ASME*, **2001**, 123, 105.
- [17] T. E. Beechem, S. Graham, P. E. Hopkins, and P. M. Norris, *Applied Physics Letters*, **2007**, 90, 1.
- [18] R. Prasher, *Applied Physics Letters*, **2009**, 94, 3.
- [19] P. E. Hopkins, J. C. Duda, and P. M. Norris, *Journal of Heat Transfer-Transactions of the Asme*, **2011**, 133, 11.
- [20] A. V. Sergeev, *Physical Review B*, **1998**, 58, 10199.
- [21] G. D. Mahan, *Physical Review B*, **2009**, 79, 1.
- [22] W. I. Choi, K. Kim, and S. Narumanchi, *J. Appl. Phys.*, **2012**, 112, 1.
- [23] R. J. Stevens, L. V. Zhigilei, and P. M. Norris, *International Journal of Heat and Mass Transfer*, **2007**, 50, 3977.
- [24] R. N. Salaway, P. E. Hopkins, P. M. Norris, and R. Stevens, *International Journal of Thermophysics*, **2008**, 29, 1987.
- [25] E. S. Landry and A. J. H. McGaughey, *Physical review B*, **2009**, 80, 11.
- [26] Z. Liang and H.-L. Tsai, *Journal of Physics: Condensed Matter*, **2011**, 23, 1.
- [27] X. Li and R. Yang, *Physical Review B*, **2012**, 86.
- [28] T. S. English, J. C. Duda, J. L. Smoyer, D. A. Jordan, P. M. Norris, and L. V. Zhigilei, *Physical review B*, **2012**, 85.

- [29] C. B. Saltonstall, C. A. Polanco, J. C. Duda, A. W. Ghosh, P. M. Norris, and P. E. Hopkins, *J. Appl. Phys.*, **2013**, 113.
- [30] Z. Tian, K. Esfarjani, and G. Chen, *Physical Review B*, **2012**, 86, 1.
- [31] M. D. Losego, M. E. Grady, N. R. Sottos, D. G. Cahill, and P. V. Braun, *Nature materials letters*, **2012**, 11, 502.
- [32] K. C. Collins, S. Chen, and G. Chen, *Applied Physics Letters*, **2010**, 97, 3.
- [33] C. Monachon and L. Weber, *J. Appl. Phys.*, **2013**, 113, 183504 1.
- [34] G. Tas, R. J. Stoner, H. J. Maris, G. W. Rubloff, G. S. Oehrlein, and J. M. Halbout, *Applied Physics Letters*, **1992**, 61, 1787.
- [35] M. D. Losego, L. Moh, K. A. Arpin, D. G. Cahill, and P. V. Braun, *Applied Physics Letters*, **2010**, 97.
- [36] P. E. Hopkins and P. M. Norris, *Applied Physics Letters*, **2006**, 89.
- [37] C. Lavoie, C. Cabral, J. M. E. Harper, G. Tas, C. J. Morath, R. J. Stoner, and H. J. Maris, *Thin Solid Films*, **2000**, 374, 42.
- [38] P. E. Hopkins, L. M. Phinney, J. R. Serrano, and T. E. Beechem, *Physical review B*, **2010**, 82, 5.
- [39] C. Monachon, M. Hojeij, and L. Weber, *Applied Physics Letters*, **2011**, 98, 1.
- [40] J. C. Duda, Y. C.-Y. P., B. M. Foley, R. Cheaito, D. L. Medlin, R. E. Jones, and P. E. Hopkins, *Applied Physics Letters*, **2013**, 102, 1.
- [41] S. Jakschik, U. Schroeder, T. Hecht, D. Krueger, G. Dollinger, A. Bergmaier, C. Luhmann, and J. W. Bartha, *Appl. Surf. Sci.*, **2003**, 211, 352.
- [42] M. M. Frank, G. D. Wilk, D. Starodub, T. Gustaffson, E. Garfunkel, Y. J. Chabal, J. Grazul, and D. A. Muller, *Applied Physics Letters*, **2005**, 86, 1.
- [43] J. A. Kittl, et al., *Microelectronic engineering*, **2009**, 86, 1789.
- [44] C. Detavernier, J. Dendooven, S. P. Sree, K. F. Ludwig, and J. A. Martens, *Chemical Society Reviews*, **2011**, 40, 5242.
- [45] P. Saint-Cast, J. Benick, D. Kania, L. Weiss, M. Hofann, J. Rentsch, R. Preu, and S. W. Glunz, *IEEE Electron Device Letters*, **2010**, 31, 695.
- [46] F. Werner, B. Veith, D. Zielke, L. Kühnemund, C. Tegenkamp, M. Seibt, R. Brendel, and J. Schmidt, *J. Appl. Phys.*, **2011**, 109, 1.
- [47] G. Dingemans and W. M. M. Kessels, *Journal of Vacuum Science and Technology A*, **2012**, 30, 040802.
- [48] S. J. Yun, Y.-W. Ko, and J. W. Lim, *Applied Physics Letters*, **2004**, 85, 4896.
- [49] A. P. Ghosh, L. J. Gerenser, J. C. M., and J. E. Fornalik, *Applied Physics Letters*, **2005**, 86, 1.
- [50] S. Ferrari, F. Perissinotti, E. Peron, L. Fumagalli, D. Natali, and M. Sampietro, *Organic Electronics*, **2007**, 8, 407.
- [51] Y. S. Jung, A. S. Cavanagh, L. A. Riley, S.-H. Kang, A. C. Dillon, M. D. Groner, S. M. George, and S.-H. Lee, *Advanced Materials*, **2010**, 22, 2172.
- [52] A. Cappella, J.-L. Battaglia, V. Schick, A. Kusiak, A. Lamperti, C. Wiemer, and B. Hay, *Advanced Engineering Materials*, **2013**, 15, 1046.
- [53] S. M. Lee, G. Matamis, D. G. Cahill, and W. P. Allen, *Microscale Thermophysical Engineering*, **1998**, 2, 31.
- [54] D. G. Cahill, *Review of Scientific Instruments*, **1990**, 61, 802.
- [55] C. Monachon and L. Weber, *Emerging Materials Research*, **2012**, 1, 89.
- [56] K. Kang, Y. K. Koh, C. Chiritescu, X. Zheng, and D. G. Cahill, *Review of Scientific Instruments*, **2008**, 79, 4.
- [57] D. G. Cahill, *Review of Scientific Instruments*, **2004**, 75, 5119.
- [58] A. Feldman, *High Temperatures - High Pressures*, **1999**, 31, 293.
- [59] X. Jaeger and H. S. Carslaw.

- [60] P. E. Hopkins, J. R. Serrano, L. M. Phinney, S. P. Kearney, T. W. Grasser, and C. T. Harris, *Journal of Heat Transfer*, **2010**, 132, 1.
- [61] Y. S. Touloukian, *Thermophysical properties of matter* (Plenum Press, New York, 1970).
- [62] P. R. W. Hudson and P. P. Phakey, *Nature*, **1977**, 269, 227.
- [63] S. M. Lee, D. G. Cahill, and T. H. Allen, *Physical review B*, **1995**, 52, 253.
- [64] A. J. Minnich, J. A. Johnson, A. J. Schmidt, K. Esfarjani, M. S. Dresselhaus, K. A. Nelson, and G. Chen, *Phys. Rev. Lett.*, **2011**, 107, 1.
- [65] J. Higbie, *American Journal of Physics*, **1991**, 59, 184.
- [66] J. C. Duda and P. E. Hopkins, *Applied Physics Letters*, **2012**, 100, 111602\_1.
- [67] I. Stark, M. Stordeur, and F. Syrowatka, *Thin Solid Films*, **1993**, 226, 185.
- [68] D. G. Cahill and R. O. Pohl, *Physical Review B*, **1987**, 35, 4067.
- [69] D. R. Haynes, N. J. Tro, and S. M. George, *J. Phys. Chem.*, **1992**, 96, 8502.
- [70] P. E. Hopkins, M. Baraket, E. V. Barnat, T. E. Beechem, S. P. Kearney, J. C. Duda, J. T. Robinson, and S. G. Walton, *Nano Letters*, **2012**, 12, 590.

Received: ((will be filled in by the editorial staff))

Revised: ((will be filled in by the editorial staff))

Published online: ((will be filled in by the editorial staff))



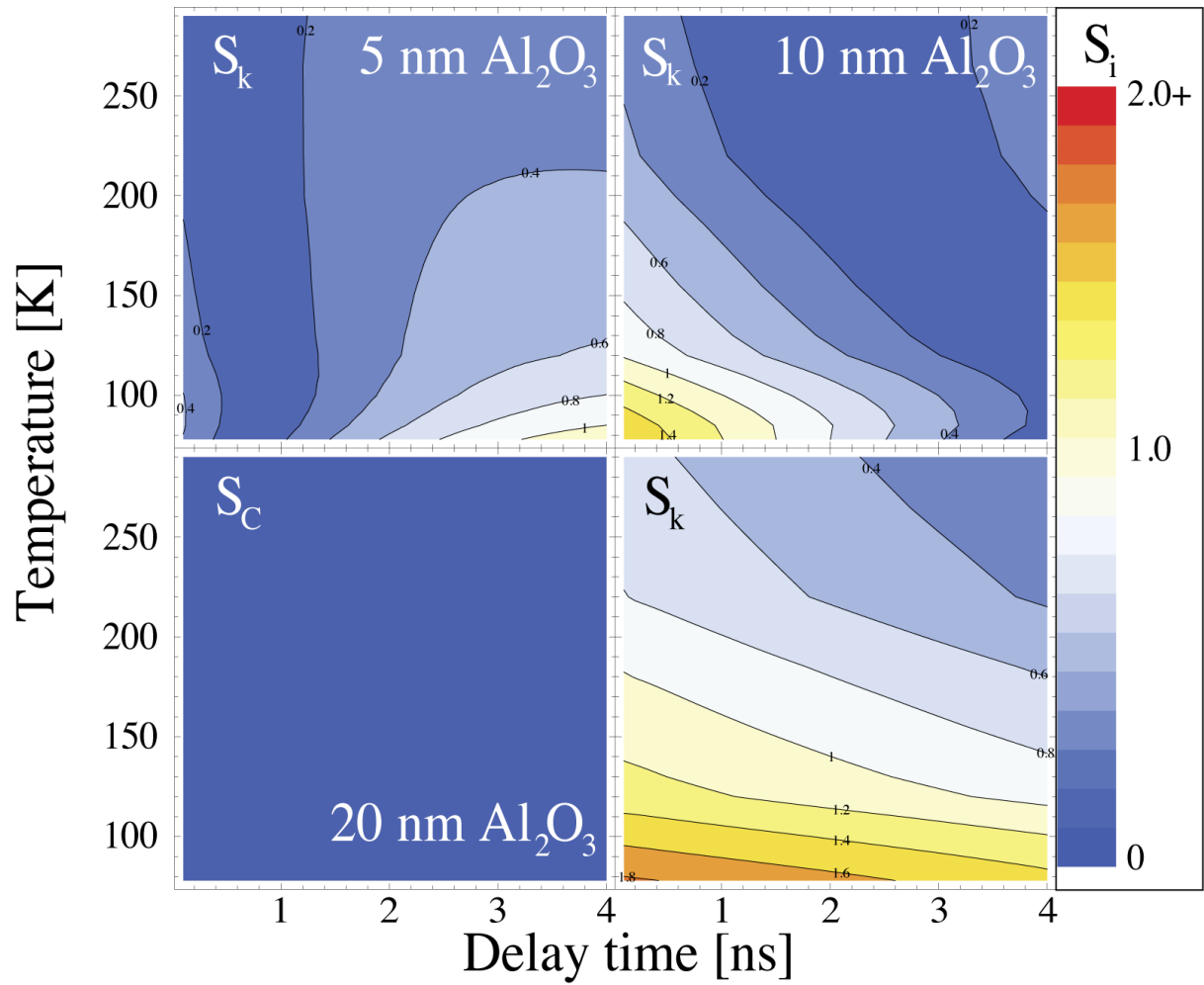


Fig. 1 Sensitivity analysis of the parameters  $k_{Al_2O_3}$  and  $C_{Al_2O_3}$  using Equation 8, as a function of both time and temperature.

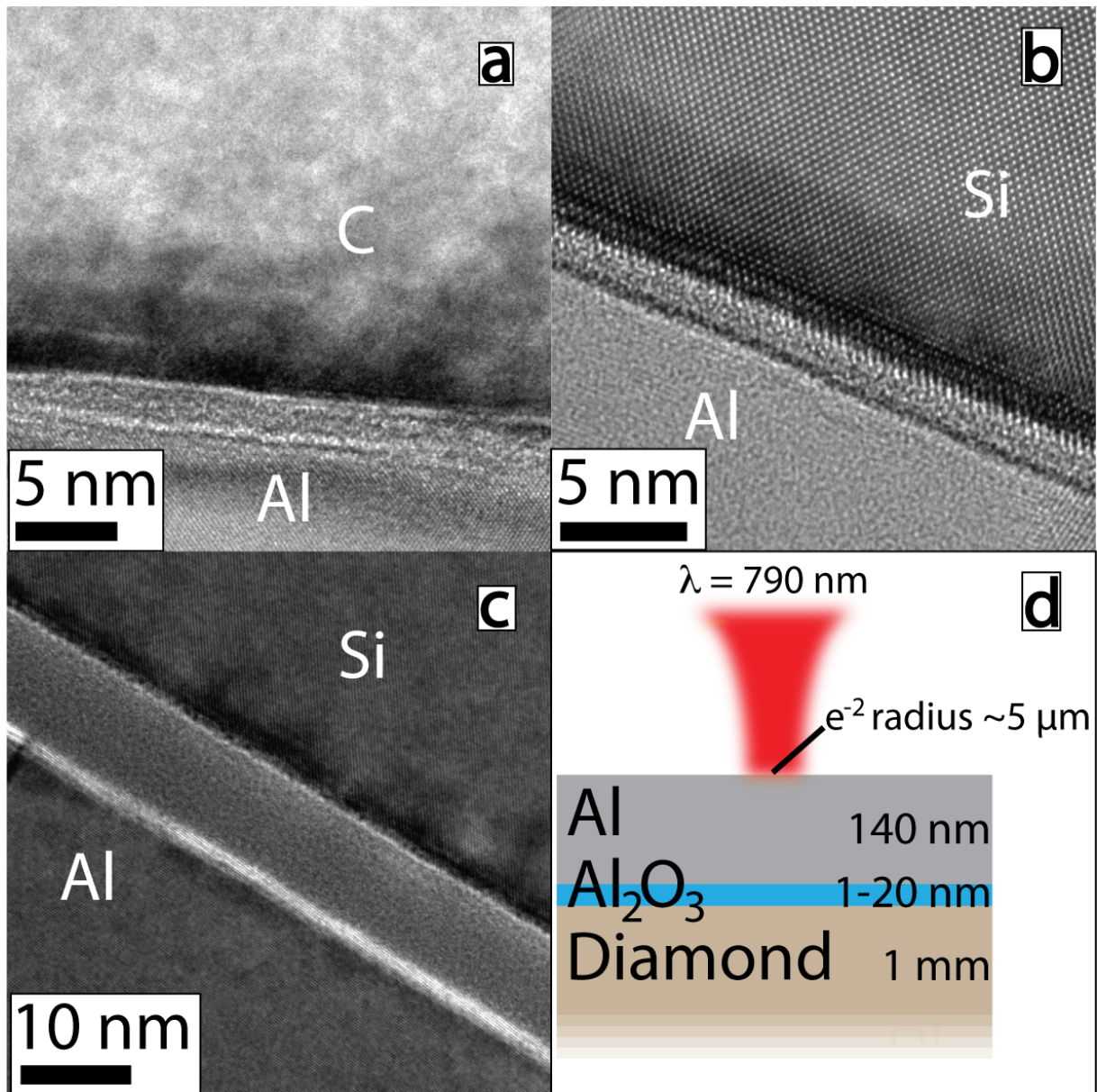


Fig. 2 Example of the images used for the  $\text{Al}_2\text{O}_3$  interlayer thickness measurements. Point a), and c) show cross section images from diamond substrate samples prepared by FIB. Point b) shows the Si substrate counterpart of a) to show that the thickness of the layer is the same on both substrates (for a 1 nm layer, value on C:  $1.8 \pm 0.3$  nm, on Si:  $1.7 \pm 0.1$  nm, for a 3 nm layer: on C:  $4.5 \pm 0.3$  nm, on Si:  $4.5 \pm 0.1$  nm, for a 5 nm layer: on C:  $6.2 \pm 0.5$  nm, on Si:  $6.2 \pm 0.1$  nm, for a 10 nm layer:  $10.0 \pm 0.1$  nm. Part d) shows a schematic diagram of the samples investigated in the case of a diamond substrate.

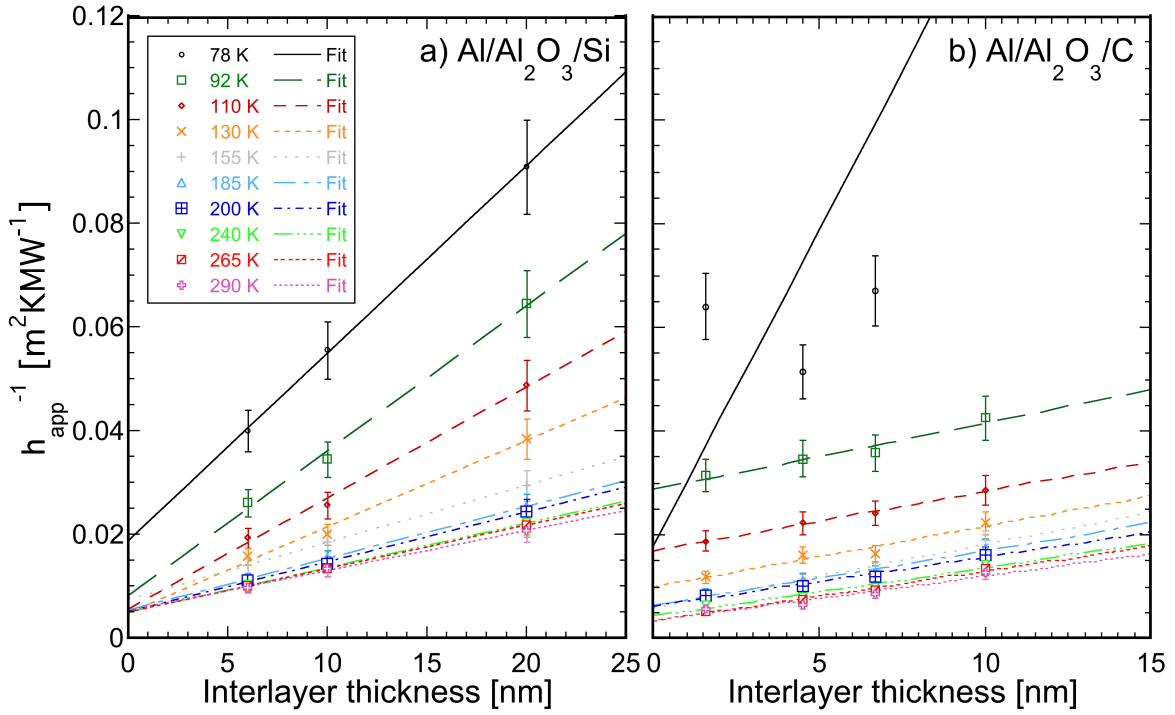


Fig. 3 Examples of fits obtained on plots of  $h_{app}^{-1}$  vs  $Al_2O_3$  interlayer thickness  $d$ , in the case of a Si (a) and a diamond (b) substrate. The error bars account for a variability of 10 % observed when measuring the same interface twice.

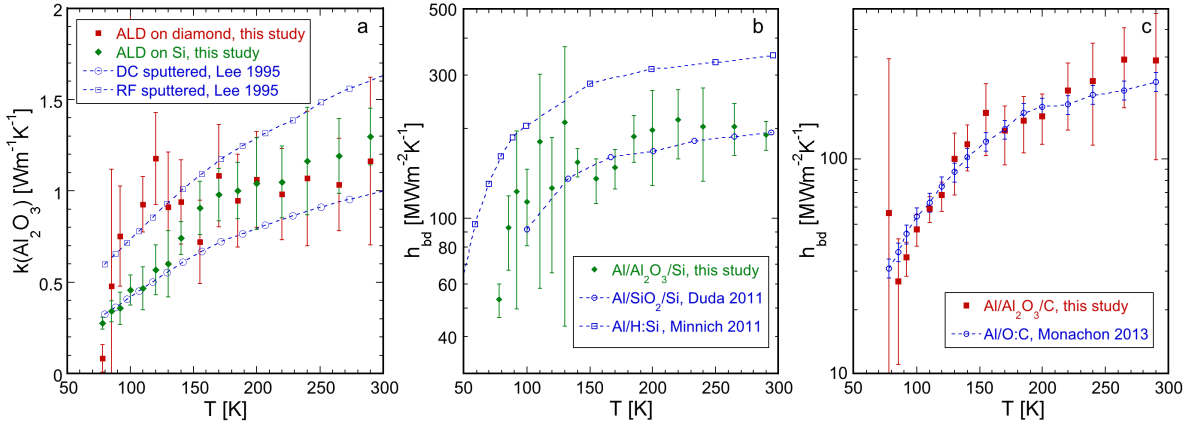


Fig. 4 Conductivities of the  $Al_2O_3$  interlayer (a) and  $Al/Al_2O_3/X$  ( $X=C, Si$ ) interfacial contributions to thermal conductance (b,c) values from the fits in **Figure 3**. The error bars account for the quality of the fit (Eq. 10 and 11) and the variability of the data. Literature from Lee et al.[57] (a), Minnich et al.[55], Duda et al.[58] (b) and Monachon and Weber [33] (c) are shown for comparison.

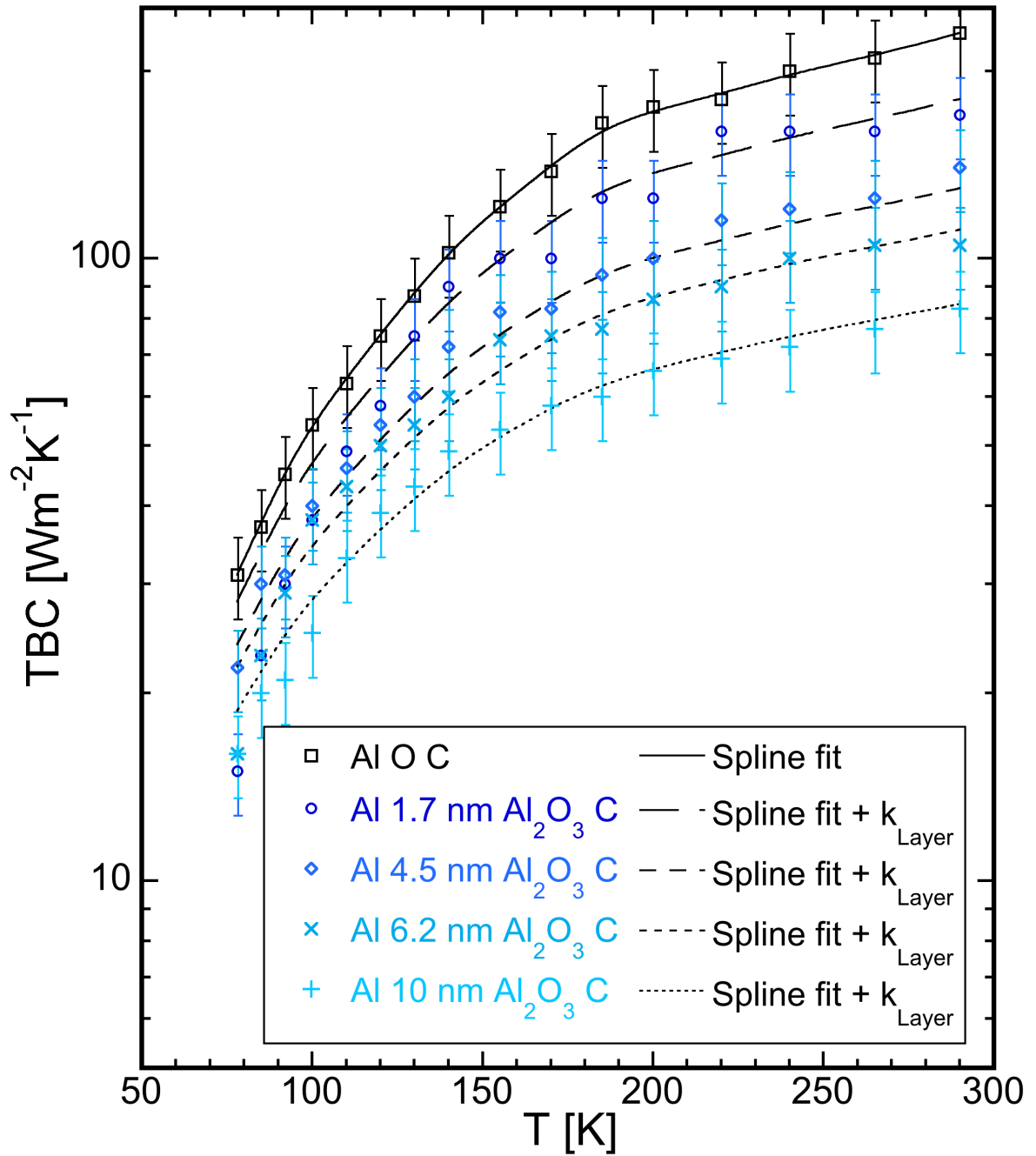


Fig. 5 Overall conductances obtained for the Al/Al<sub>2</sub>O<sub>3</sub>/O:C interfaces, directly measured as conductances (the heat capacity of Al<sub>2</sub>O<sub>3</sub> was accounted for by artificially increasing the Al layer thickness in the fitting model). The top black curves is a spline fit of the TBC values obtained on the Al/O:C interfaces (data taken from Ref. [33]) and the other lines consist in the same curve, modified to account for the thermal conductivity of the Al<sub>2</sub>O<sub>3</sub> interlayer.

The table of contents entry should approximately one hundred words, written in the present tense, and refer to the chosen figure.

Title ((no stars))

ToC figure ((48 mm broad))

Supporting Information should be included here (for submission only; for publication, please provide Supporting Information as a separate PDF file).

- [1] D. G. Cahill, F. K. Wayne, K. E. Goodson, G. D. Mahan, A. Majumdar, H. J. Maris, R. Merlin, and S. R. Philipot, *Applied Physics Reviews*, **2003**, 93, 793.
- [2] E. Pop, *Nano Research*, **2010**, 3, 147.
- [3] R. M. Costescu, D. G. Cahill, F. H. Fabreguette, Z. A. Sechrist, and S. M. George, *Science*, **2004**, 303, 989.
- [4] C. Chiritescu, D. G. Cahill, N. Nguyen, D. Johnson, A. Bodapati, P. Keblinski, and P. Zschack, *Science*, **2007**, 315, 351.
- [5] W. S. Capinski, H. J. Maris, T. Ruf, M. Cardona, K. Ploog, and D. S. Katzer, *Physical Review B*, **1999**, 59, 8105.
- [6] C. Dames, *Nature nanotechnology*, **2012**, 7, 82.
- [7] M. N. Luckyanova, et al., *Science*, **2012**, 338, 336.
- [8] E. T. Swartz and R. O. Pohl, *Reviews of Modern Physics*, **1989**, 61, 605.
- [9] R. J. Stoner and H. J. Maris, *Physical Review B*, **1993**, 48, 16373.
- [10] S.-M. Lee and D. G. Cahill, *Microscale Thermophysical Engineering*, **1997**, 1, 47.
- [11] R. M. Costescu, M. D. Wall, and D. G. Cahill, *Physical Review B*, **2003**, 67, 1.
- [12] H.-K. Lyeo and D. G. Cahill, *Physical Review B*, **2006**, 73, 144301 1.
- [13] P. E. Hopkins, P. M. Norris, and R. J. Stevens, *Journal of Heat Transfer*, **2008**, 130, 022401.
- [14] W. A. Little, *Canadian Journal of Physics*, **1959**, 37, 334.
- [15] D. A. Young and H. J. Maris, *Physical Review B*, **1989**, 40, 3685.
- [16] R. S. Prasher and P. E. Phelan, *Journal of heat Transfer-Transactions of the ASME*, **2001**, 123, 105.
- [17] T. E. Beechem, S. Graham, P. E. Hopkins, and P. M. Norris, *Applied Physics Letters*, **2007**, 90, 1.
- [18] R. Prasher, *Applied Physics Letters*, **2009**, 94, 3.
- [19] P. E. Hopkins, J. C. Duda, and P. M. Norris, *Journal of Heat Transfer-Transactions of the Asme*, **2011**, 133, 11.
- [20] A. V. Sergeev, *Physical Review B*, **1998**, 58, 10199.
- [21] G. D. Mahan, *Physical Review B*, **2009**, 79, 1.
- [22] W. I. Choi, K. Kim, and S. Narumanchi, *J. Appl. Phys.*, **2012**, 112, 1.
- [23] R. J. Stevens, L. V. Zhigilei, and P. M. Norris, *International Journal of Heat and Mass Transfer*, **2007**, 50, 3977.
- [24] R. N. Salaway, P. E. Hopkins, P. M. Norris, and R. Stevens, *International Journal of Thermophysics*, **2008**, 29, 1987.
- [25] E. S. Landry and A. J. H. McGaughey, *Physical review B*, **2009**, 80, 11.
- [26] Z. Liang and H.-L. Tsai, *Journal of Physics: Condensed Matter*, **2011**, 23, 1.
- [27] X. Li and R. Yang, *Physical Review B*, **2012**, 86.
- [28] T. S. English, J. C. Duda, J. L. Smoyer, D. A. Jordan, P. M. Norris, and L. V. Zhigilei, *Physical review B*, **2012**, 85.
- [29] C. B. Saltonstall, C. A. Polanco, J. C. Duda, A. W. Ghosh, P. M. Norris, and P. E. Hopkins, *J. Appl. Phys.*, **2013**, 113.
- [30] Z. Tian, K. Esfarjani, and G. Chen, *Physical Review B*, **2012**, 86, 1.
- [31] M. D. Losego, M. E. Grady, N. R. Sottos, D. G. Cahill, and P. V. Braun, *Nature materials letters*, **2012**, 11, 502.
- [32] K. C. Collins, S. Chen, and G. Chen, *Applied Physics Letters*, **2010**, 97, 3.
- [33] C. Monachon and L. Weber, *J. Appl. Phys.*, **2013**, 113, 183504 1.
- [34] G. Tas, R. J. Stoner, H. J. Maris, G. W. Rubloff, G. S. Oehrlein, and J. M. Halbout, *Applied Physics Letters*, **1992**, 61, 1787.

- [35] M. D. Losego, L. Moh, K. A. Arpin, D. G. Cahill, and P. V. Braun, *Applied Physics Letters*, **2010**, 97.
- [36] P. E. Hopkins and P. M. Norris, *Applied Physics Letters*, **2006**, 89.
- [37] C. Lavoie, C. Cabral, J. M. E. Harper, G. Tas, C. J. Morath, R. J. Stoner, and H. J. Maris, *Thin Solid Films*, **2000**, 374, 42.
- [38] P. E. Hopkins, L. M. Phinney, J. R. Serrano, and T. E. Beechem, *Physical review B*, **2010**, 82, 5.
- [39] C. Monachon, M. Hojeij, and L. Weber, *Applied Physics Letters*, **2011**, 98, 1.
- [40] J. C. Duda, Y. C.-Y. P., B. M. Foley, R. Cheaito, D. L. Medlin, R. E. Jones, and P. E. Hopkins, *Applied Physics Letters*, **2013**, 102, 1.
- [41] S. Jakschik, U. Schroeder, T. Hecht, D. Krueger, G. Dollinger, A. Bergmaier, C. Luhmann, and J. W. Bartha, *Appl. Surf. Sci.*, **2003**, 211, 352.
- [42] M. M. Frank, G. D. Wilk, D. Starodub, T. Gustaffson, E. Garfunkel, Y. J. Chabal, J. Grazul, and D. A. Muller, *Applied Physics Letters*, **2005**, 86, 1.
- [43] J. A. Kittl, et al., *Microelectronic engineering*, **2009**, 86, 1789.
- [44] C. Detavernier, J. Dendooven, S. P. Sree, K. F. Ludwig, and J. A. Martens, *Chemical Society Reviews*, **2011**, 40, 5242.
- [45] P. Saint-Cast, J. Benick, D. Kania, L. Weiss, M. Hofann, J. Rentsch, R. Preu, and S. W. Glunz, *IEEE Electron Device Letters*, **2010**, 31, 695.
- [46] F. Werner, B. Veith, D. Zielke, L. Kühnemund, C. Tegenkamp, M. Seibt, R. Brendel, and J. Schmidt, *J. Appl. Phys.*, **2011**, 109, 1.
- [47] G. Dingemans and W. M. M. Kessels, *Journal of Vacuum Science and Technology A*, **2012**, 30, 040802.
- [48] S. J. Yun, Y.-W. Ko, and J. W. Lim, *Applied Physics Letters*, **2004**, 85, 4896.
- [49] A. P. Ghosh, L. J. Gerenser, J. C. M., and J. E. Fornalik, *Applied Physics Letters*, **2005**, 86, 1.
- [50] S. Ferrari, F. Perissinotti, E. Peron, L. Fumagalli, D. Natali, and M. Sampietro, *Organic Electronics*, **2007**, 8, 407.
- [51] Y. S. Jung, A. S. Cavanagh, L. A. Riley, S.-H. Kang, A. C. Dillon, M. D. Groner, S. M. George, and S.-H. Lee, *Advanced Materials*, **2010**, 22, 2172.
- [52] A. Cappella, J.-L. Battaglia, V. Schick, A. Kusiak, A. Lamperti, C. Wiemer, and B. Hay, *Advanced Engineering Materials*, **2013**, 15, 1046.
- [53] S. M. Lee, G. Matamis, D. G. Cahill, and W. P. Allen, *Microscale Thermophysical Engineering*, **1998**, 2, 31.
- [54] D. G. Cahill, *Review of Scientific Instruments*, **1990**, 61, 802.
- [55] C. Monachon and L. Weber, *Emerging Materials Research*, **2012**, 1, 89.
- [56] K. Kang, Y. K. Koh, C. Chirutescu, X. Zheng, and D. G. Cahill, *Review of Scientific Instruments*, **2008**, 79, 4.
- [57] D. G. Cahill, *Review of Scientific Instruments*, **2004**, 75, 5119.
- [58] A. Feldman, *High Temperatures - High Pressures*, **1999**, 31, 293.
- [59] X. Jaeger and H. S. Carslaw.
- [60] P. E. Hopkins, J. R. Serrano, L. M. Phinney, S. P. Kearney, T. W. Grasser, and C. T. Harris, *Journal of Heat Transfer*, **2010**, 132, 1.
- [61] Y. S. Touloukian, *Thermophysical properties of matter* (Plenum Press, New York, 1970).
- [62] P. R. W. Hudson and P. P. Phakey, *Nature*, **1977**, 269, 227.
- [63] S. M. Lee, D. G. Cahill, and T. H. Allen, *Physical review B*, **1995**, 52, 253.
- [64] A. J. Minnich, J. A. Johnson, A. J. Schmidt, K. Esfarjani, M. S. Dresselhaus, K. A. Nelson, and G. Chen, *Phys. Rev. Lett.*, **2011**, 107, 1.
- [65] J. Higbie, *American Journal of Physics*, **1991**, 59, 184.
- [66] J. C. Duda and P. E. Hopkins, *Applied Physics Letters*, **2012**, 100, 111602\_1.

- [67] I. Stark, M. Stordeur, and F. Syrowatka, *Thin Solid Films*, **1993**, 226, 185.
- [68] D. G. Cahill and R. O. Pohl, *Physical Review B*, **1987**, 35, 4067.
- [69] D. R. Haynes, N. J. Tro, and S. M. George, *J. Phys. Chem.*, **1992**, 96, 8502.
- [70] P. E. Hopkins, M. Baraket, E. V. Barnat, T. E. Beechem, S. P. Kearney, J. C. Duda, J. T. Robinson, and S. G. Walton, *Nano Letters*, **2012**, 12, 590.